Supporting Information for

Improving robustness and training efficiency of machine-learned potentials by incorporating short-range empirical potentials

Zihan Yan[1,2] ⓘ, Zheyong Fan[3] ⓘ, and Yizhou Zhu[2,*] ⓘ

[1]School of Materials Science and Engineering, Zhejiang University, Hangzhou, Zhejiang 310027, China
[2]Research Center for Industries of the Future and School of Engineering, Westlake University, 600 Dunyu Road, Hangzhou, Zhejiang 310030, China
[3]College of Physical Science and Technology, Bohai University, Jinzhou 121013, China
*Corresponding author: Yizhou Zhu (zhuyizhou@westlake.edu.cn)

NEP Hyperparameters. We employ the fourth generation of NEP model proposed by Fan *et al.* to construct our interatomic potential for LLZO. The training hyperparameters are listed in Tab. S1. A cutoff radius of 6 Å and 4 Å was adopted for the radial and angular components, respectively. The expansion order for three-body and four-body angular terms was $l_{max}^{3b} = 4$ and $l_{max}^{4b} = 2$. We performed 1×10^5 iterations to obtain a converged NEP4 model. The evolution of various terms in the loss function and the parity plot of energies, forces, and stresses can be found in Fig. S1–6.

Table S1: Hyperparameters for the NEP model.

Parameter	Value	Parameter	Value
r_c^R	6 Å	r_c^A	4 Å
n_{max}^R	4	n_{max}^A	4
N_{bas}^R	8	N_{bas}^A	8
l_{max}^{3b}	4	l_{max}^{4b}	2
N_{neu}	30	N_{pop}	50
λ_1	0.0363352	λ_2	0.0363352
λ_e	1	λ_f	1
λ_v	0.1	N_{batch}	200

Table S2: Exploration iterations for Garnet *without ZBL* potential. The Failure Ratio (FR) represents the fraction of unphysical structures within the trajectory relative to the total structure count. Unphysical structures are filtered out during the sampling process. The force field will only be updated if N_{samp} is greater than 20. min_distance=0.008 is used in the Farthest Point Sample.

Iter	t (ps)	Sample1	Sample2	Sample3	Sample4	N_{samp}	FR (%)	Update?
1	20	100-400K	100-400K	500-800K	500-800K	96	0%	yes
2	50	100-400K	100-400K	500-800K	500-800K	30	0%	yes
3	100	100-400K	500-800K	500-800K	500-800K	68	0%	yes
4	500	500-800K	500-800K	500-800K	500-800K	5	0%	no
5	20	800-1000K	800-1000K	800-1000K	800-1000K	43	0%	yes
6	50	800-1000K	800-1000K	1000-1200K	1000-1200K	231	8.8%	yes
7	50	800-1000K	800-1000K	1000-1200K	1000-1200K	8	0%	no
8	100	800-1000K	800-1000K	1000-1200K	1000-1200K	21	1.6%	yes
9	100	800-1000K	800-1000K	1000-1200K	1000-1200K	145	0%	yes
10	500	800-1000K	800-1000K	1000-1200K	1000-1200K	31	10.6%	yes
11	500	800-1000K	800-1000K	1000-1200K	1000-1200K	8	0%	no
12	500	1000-1200K	1000-1200K	1000-1200K	1000-1200K	16	0%	no
13								yes

Table S3: Exploration iterations for Garnet *with ZBL* potential. The Failure Ratio (FR) represents the fraction of unphysical structures within the trajectory relative to the total structure count. The force field will only be updated if N_{samp} is greater than 20. min_distance=0.01 is used in the Farthest Point Sample.

Iter	t (ps)	Sample1	Sample2	Sample3	Sample4	N_{samp}	FR (%)	Update?
1	500	100-400K	100-400K	100-400K	100-400K	12	0%	no
2	500	500-800K	500-800K	500-800K	500-800K	51	0%	yes
3	500	800-1200K	800-1200K	800-1200K	800-1200K	44	0%	yes

Table S4: Exploration iterations for Garnet *without ZBL* potential. The Failure Ratio (FR) represents the fraction of unphysical structures within the trajectory relative to the total structure count. Unphysical structures are filtered out during the sampling process. The force field will only be updated if N_{samp} is greater than 20. min_distance=0.01 is used in the Farthest Point Sample.

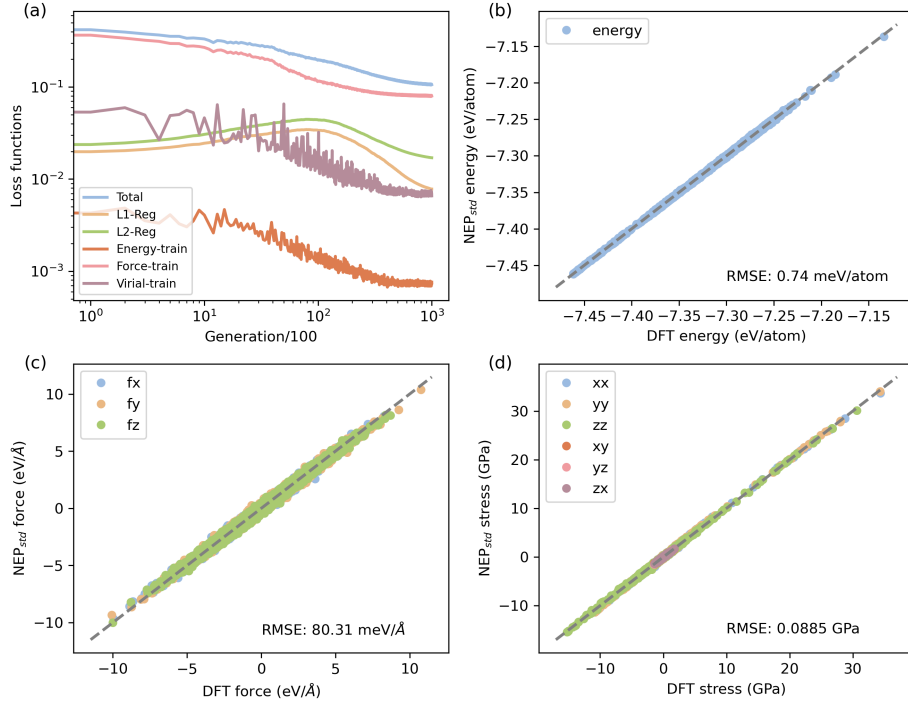| Iter	t (ps)	Sample1	Sample2	Sample3	Sample4	N_{samp}	FR (%)	Update?
1	500	100-400K	100-400K	100-400K	100-400K	10	0%	no
2	500	500-800K	500-800K	500-800K	500-800K	22	19.9%	yes
3	500	800-1200K	800-1200K	800-1200K	800-1200K	29	57.9%	yes

Figure S1: (a) Evolution of the various terms in the loss function. (b) Energy, (c) force, and (d) stress values from the NEP$_{std}$ model, in comparison to the DFT reference data.
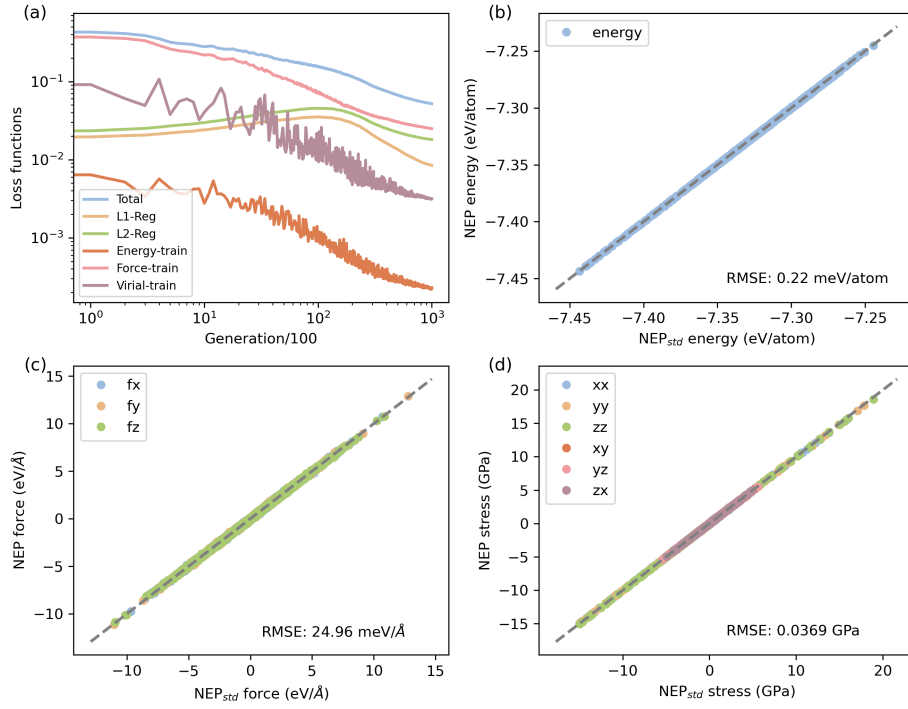

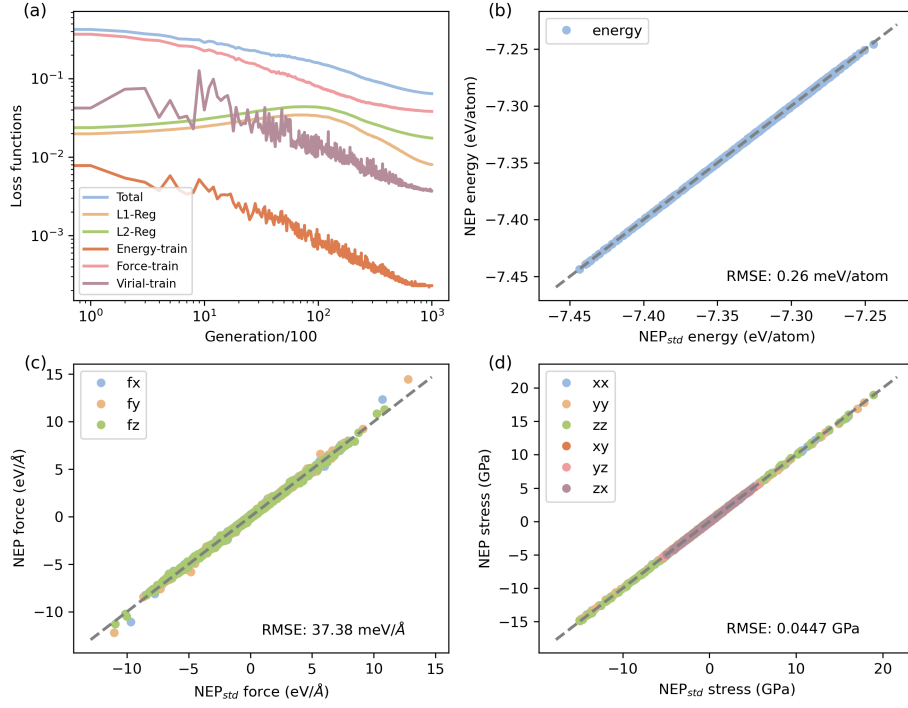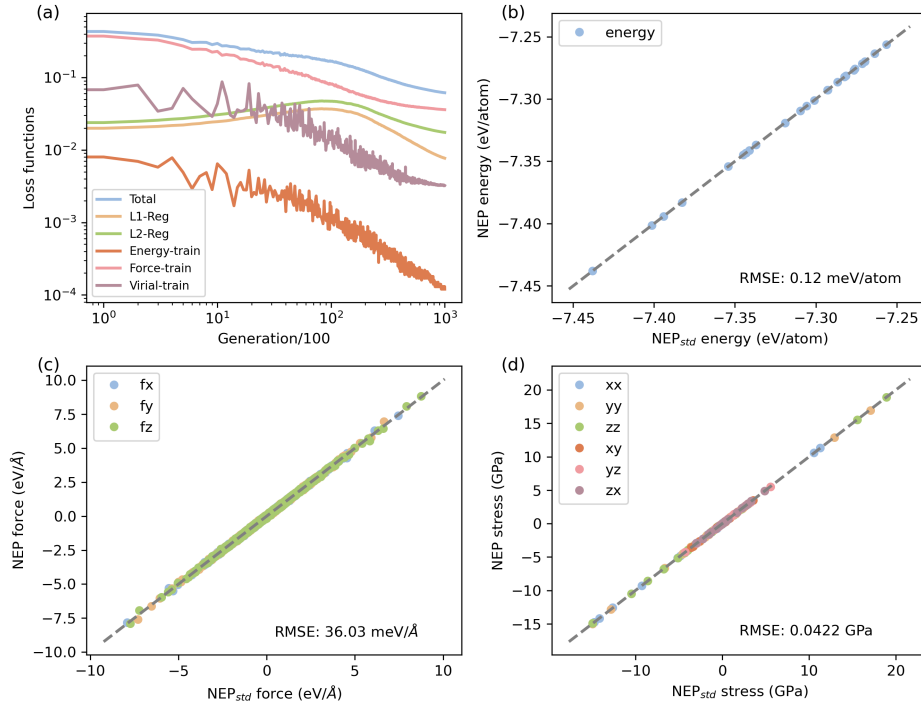
Figure S2: (a) Evolution of the various terms in the loss function. (b) Energy, (c) force, and (d) stress values from the NEP$_{802}$ model, in comparison to the NEP$_{std}$ reference data.
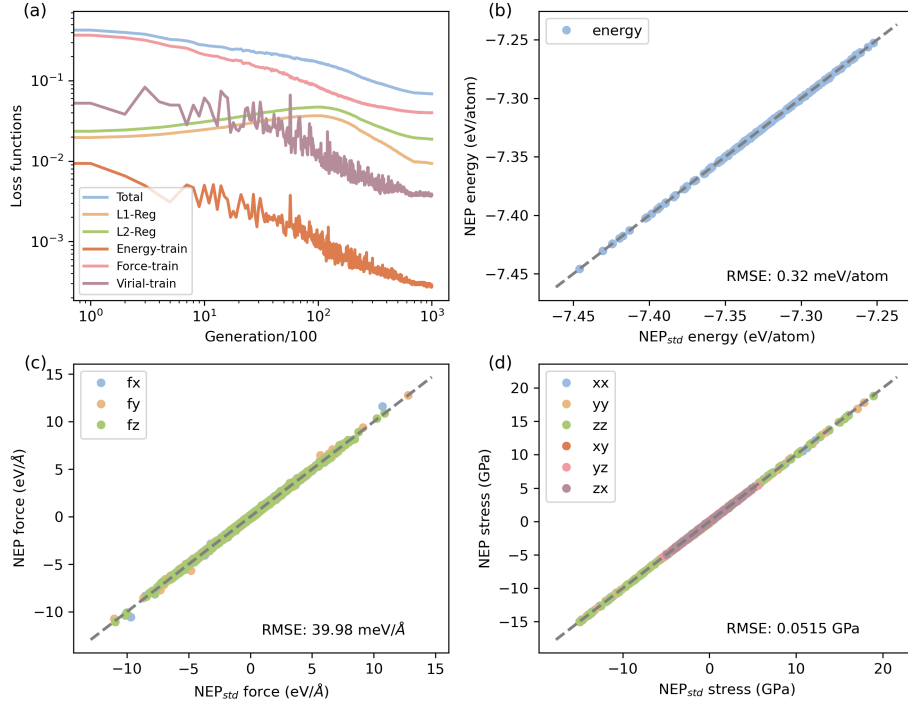
Figure S3: (a) Evolution of the various terms in the loss function. (b) Energy, (c) force, and (d) stress values from the NEP_{802}-ZBL model, in comparison to the NEP_{std} reference data.

Figure S4: (a) Evolution of the various terms in the loss function. (b) Energy, (c) force, and (d) stress values from the NEP_{25}-ZBL model, in comparison to the NEP_{std} reference data.

Figure S5: (a) Evolution of the various terms in the loss function. (b) Energy, (c) force, and (d) stress values from the NEP$_{207}$-ZBL model, in comparison to the NEP$_{std}$ reference data.
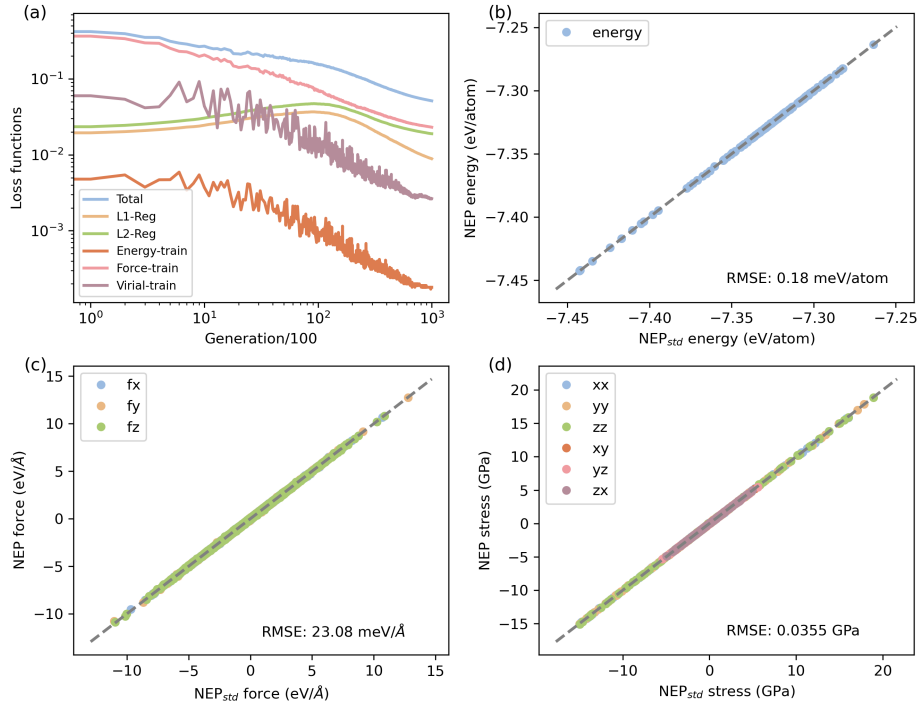

Figure S6: (a) Evolution of the various terms in the loss function. (b) Energy, (c) force, and (d) stress values from the NEP$_{161}$ model, in comparison to the NEP$_{std}$ reference data.
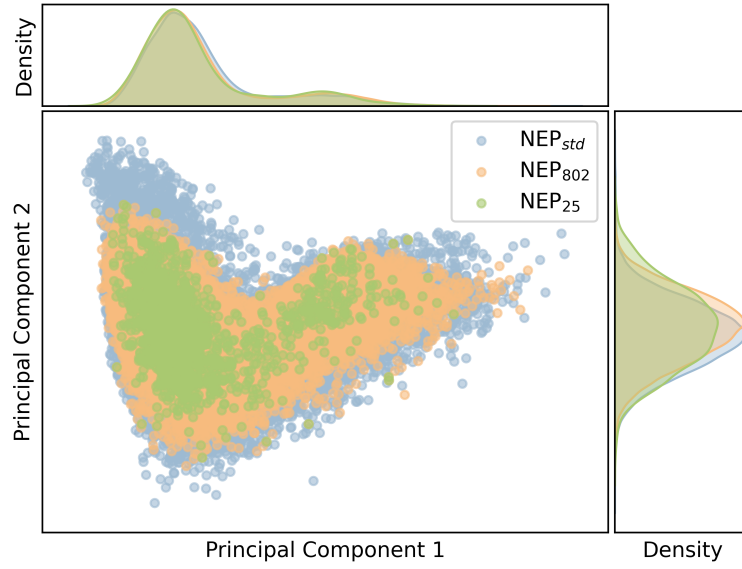
Figure S7: Principal Component Analysis of Li^+ high-dimensional descriptors in different training sets.
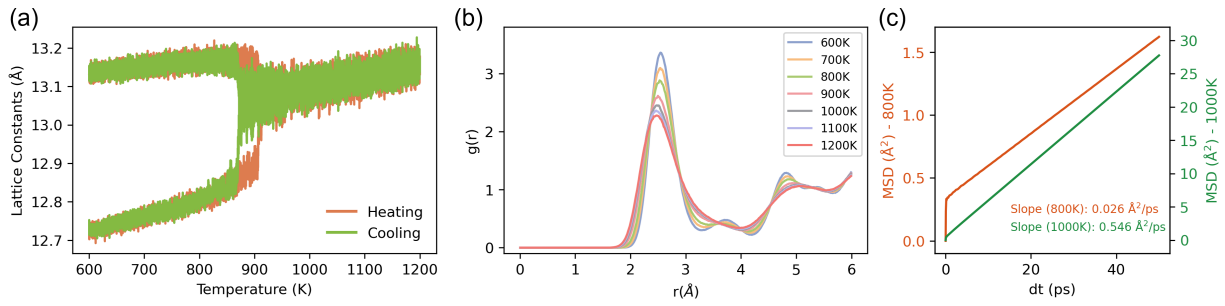

Figure S8: (a-c) show the various properties calculated using NEP_{207}-ZBL, including (a) the lattice evolution of LLZO during heating and cooling processes, (b) the radial distribution function of Li^+-Li^+ at $600 - 1200$ K, and (c) the mean square displacements of Li^+ ions over correlation times at 800 K and 1000 K.